Inorg. Chem. **2008**, *47*, 9958−9964

Tetravalent Silicon Connectors $Me_nSi(p\text{-}C_6H_4CO_2H)_{4-n}$ (n = 0, 1, 2) for the Construction of Metal−Organic Frameworks

R. P. Davies,* R. J. Less,† P. D. Lickiss,* K. Robertson, and A. J. P. White

Department of Chemistry, Imperial College London, South Kensington, London SW7 2AZ, United Kingdom

Received June 25, 2008

A series of silicon-centered connecting units, $Me_nSi(p\text{-}C_6H_4CO_2H)_{4-n}$ (n = 0, 1, 2), have been prepared and their coordination polymers with Zn(II) metal atoms studied. The tetra-acid **L1** (n = 0) acts as a tetrahedral node and reacts with Zn(II) centers to give **1**, a novel interpenetrating 3D network containing distorted tetrahedral bimetallic secondary building units (SBUs). The triacid **L2** (n = 1) acts as a trigonal pyramidal node and forms an intercalated 2D layered network, **2**, with Zn(II) ions, containing distorted octahedral tetranuclear SBUs. Last, the bent diacid **L3** (n = 2) reacts with Zn(II) centers to give **3**, a corrugated 2D layered structure containing 1D zinc hydroxo chains. Together these three new coordination polymers demonstrate the potential versatility of tetravalent silicon containing connecting ligands for metal−organic framework construction.

Introduction

There is currently much interest in the chemistry of metal-containing coordination polymers and metal−organic frameworks (MOFs), primarily driven by their potential applications in fields as diverse as gas storage, catalysis, nonlinear optics, electronics, ion exchange, and enantioselective separations.[1−10] Many MOFs are constructed from simple commercially available bent or linear dicarboxylic acids, which act as connecting units between metal-based nodes or clusters—often defined as secondary building units or SBUs—to give a three-dimensional network structure. The desire to better control the physical and chemical properties of the resultant networks has motivated recent research into the systematic design of new connecting ligands with specifically tailored dimensionality or pendant functional groups.

We have been interested in the preparation of novel silicon-based connecting units and their use in the construction of metal-containing coordination polymers.[11−15] Tetrahedral silicon centers are in general more synthetically accessible than their carbon equivalents and are thus promising candidates for a series of new connecting units with easily modifiable structural and chemical properties. In addition, when compared to their carbon analogues, the longer bond lengths to silicon in these molecules and their increased bond angle flexibility at silicon and decreased conformational rigidity have been shown in some cases to lead to the formation of coordination polymers with novel topological and structural forms.[11−15]

Recent examples of silicon-based connecting units being used for the construction of MOF materials includes work

* Authors to whom all correspondence should be addressed: E-mail: r.davies@imperial.ac.uk (R.P.D.).

† Current address: The University Chemical Laboratory, University of Cambridge, Lensfield Road, Cambridge CB2 1EW, United Kingdom.

(1) Ferey, G. *Chem. Soc. Rev.* **2008**, *37*, 191–214.
(2) James, S. L. *Chem. Soc. Rev.* **2003**, *32*, 276–288.
(3) Janiak, C. *Dalton Trans.* **2003**, 2781–2804.
(4) Bradshaw, D.; Claridge, J. B.; Cussen, E. J.; Prior, T. J.; Rosseinsky, M. J. *Acc. Chem. Res.* **2005**, *38*, 273–282.
(5) Papaefstathiou, G. S.; MacGillivray, L. R. *Coord. Chem. Rev.* **2003**, *246*, 169–184.
(6) Eddaoudi, M.; Moler, D. B.; Li, H. L.; Chen, B. L.; Reineke, T. M.; O'Keeffe, M.; Yaghi, O. M. *Acc. Chem. Res.* **2001**, *34*, 319–330.
(7) Rowsell, J. L. C.; Yaghi, O. M. *Microporous Mesoporous Mater.* **2004**, *73*, 3–14.
(8) Rosseinsky, M. J. *Microporous Mesoporous Mater.* **2004**, *73*, 15–30.
(9) Mori, W.; Takamizawa, S.; Kato, C. N.; Ohmura, T.; Sato, T. *Microporous Mesoporous Mater.* **2004**, *73*, 31–46.
(10) Xu, Z. *Coord. Chem. Rev.* **2006**, *250*, 2745–2757.
(11) Fereday, A.; Goodgame, D. M. L.; Lickiss, P. D.; Rooke, S. J.; White, A. J. P.; Williams, D. J. *Inorg. Chem. Commun.* **2002**, *5*, 805–807.
(12) Goodgame, D. M. L.; Lickiss, P. D.; Rooke, S. J.; White, A. J. P.; Williams, D. J. *Inorg. Chim. Acta* **2001**, *324*, 218–231.
(13) Goodgame, D. M. L.; Lickiss, P. D.; Rooke, S. J.; White, A. J. P.; Williams, D. J. *Inorg. Chim. Acta* **2003**, *343*, 61–73.
(14) Goodgame, D. M. L.; Lickiss, P. D.; Rooke, S. J.; White, A. J. P.; Williams, D. J. In *Organosilicon Chemistry V*; Auner, N., Weis, J., Eds.; Wiley-VCH: New York, 2003, pp. 447−450.
(15) Goodgame, D. M. L.; Kealey, S.; Lickiss, P. D.; White, A. J. P. *J. Mol. Struct.* **2008**, in press. DOI: 10.1016/j.molstruc.2008.05.013.

10.1021/ic801174d CCC: $40.75
Published on Web 10/01/2008

by Tilley and Liu on Ag(I)-[16] and Ti(IV)[17]-containing 3D MOFs with $Si(p\text{-}C_6H_4CN)_4$ tetrahedral building blocks, research by Jung et al. on Ag(I) coordination polymers with bidentate $Me_2Si(4\text{-}C_5H_4N)_2$ ligands,[18,19] and most recently a report by Lambert et al. on a 3D MOF constructed from $Si(p\text{-}C_6H_4CO_2H)_4$ and Zn(II) centers.[20] In addition, 3D hydrogen-bonded assemblies have been reported for $Si(p\text{-}C_6H_4CO_2H)_4$[21,22] and $Si(p\text{-}C_6H_4B(OH)_2)_4$;[23] Yaghi and coworkers[24] have used the condensation reaction of $Si(p\text{-}C_6H_4B(OH)_2)_4$ to yield a 3D covalent organic framework, and Kaskel et al.[25] have prepared a microporous polysilane material from the lithiation of $Si(p\text{-}C_6H_4Br)_4$. We now report on a new 3D-MOF material prepared from the tetracarboxylate ligand $Si(p\text{-}C_6H_4CO_2H)_4$, as well as on the synthesis and application of the related tri- and dicarboxylate connectors, $MeSi(p\text{-}C_6H_4CO_2H)_3$ and $Me_2Si(p\text{-}C_6H_4CO_2H)_2$, for the construction of novel 2D network materials.

Experimental Section

All reactions involving *n*-BuLi were carried out in oven-dried glassware and were performed under an atmosphere of nitrogen. Diethyl ether and THF were dried by distillation over sodium metal prior to use. **L1** was prepared according to literature procedures.[26] All other reagents were commercial products that were used without further purification. NMR spectra were recorded on a Bruker AV-400 spectrometer and mass spectra on a Micromass AutoSpec Premier. Microanalytical data were obtained from the Science Technical Support Unit, London Metropolitan University.

Synthesis of $MeSi(p\text{-}C_6H_4Br)_3$. *n*-BuLi (2.5 M in hexanes, 17 mL, 42 mmol) was added to a solution of 1,4-dibromobenzene (10.0 g, 42 mmol) in 100 mL Et_2O at 0 °C and stirred for 30 min. Trichloromethylsilane (1.6 mL, 14 mmol) was then added dropwise and the reaction mixture heated at reflux for 2 h. After being quenched with 50 mL of H_2O, the organic layer was separated, washed with brine, and dried over anhydrous $MgSO_4$. Removal of the solvents under a vacuum yielded 10.2 g of a yellow oil, to which was added a 1:1 mixture of dichloromethane and hexane. This solution was filtered through a plug of silica and the solvents removed to give the crude product. Recrystallization from hexane gave pure $MeSi(p\text{-}C_6H_4Br)_3$ (4.75 g, 66%). Mp: 106−112 °C. ^{1}H NMR ($CDCl_3$) δ/ppm: 7.50 (d, J = 7.4 Hz, 6H, ArH), 7.30 (d, J = 7.4 Hz, 6H, ArH), 0.80 (s, 3H, CH_3). ^{13}C NMR ($CDCl_3$) δ/ppm: 136.7 (ArH), 133.8 (Ar), 131.3 (ArH), 124.9 (Ar), −3.9 (CH_3). *m/e* (+EI): 512 (M^+), 497 ($M^+ - CH_3$), 417 ($M^+ - CH_3 - Br$), 355 ($M^+ - C_6H_4Br$). Anal. calcd %: C, 44.65; H, 2.96. Found: C, 44.69; H, 3.00. IR (nujol mull): 1912, 1570, 1550, 1478, 1340, 1304, 1254, 1186, 1111, 1068, 1010, 968, 950, 836, 814, 808, 783, 741, 722 cm^{-1}.

Synthesis of $Me_2Si(p\text{-}C_6H_4Br)_2$. A solution of *n*-BuLi (2.5 M in hexanes, 34 mL, 84 mmol) in 40 mL of Et_2O was added dropwise to a solution of 1,4-dibromobenzene (20.0 g, 84 mmol) in 60 mL of Et_2O at 0 °C and stirred at this temperature for 1 h. Dichlorodimethylsilane (5.1 mL, 42 mmol) was then added dropwise and the reaction mixture stirred for 12 h at room temperature. The reaction was then quenched by the addition of 50 mL of 1 M HCl and the organic layer separated, washed with brine, and dried over magnesium sulfate. Upon storage at −20 °C for 24 h, colorless crystals of $Me_2Si(p\text{-}C_6H_4Br)_2$ were obtained (8.54 g, 55%). Mp: 78 °C. ^{1}H NMR ($CDCl_3$) δ/ppm: 7.51 (d, 4H, J = 8.1 Hz, ArH), 7.36 (d, 4H, J = 8.2 Hz, ArH), 0.55 (s, 6H, Me) ppm. ^{13}C NMR ($CDCl_3$) δ/ppm: 136.4 (Ar), 135.7 (ArH), 131.1 (ArH), 124.3 (Ar), −2.5 (CH_3). *m/e* (+EI): 370 (M^+), 355 ($M^+ - CH_3$), 290, ($M^+ -$ Br), 275 ($M^+ - CH_3 -$ Br), 259 ($M^+ - 2CH_3 -$ Br), 215 ($M^+ - C_6H_4Br$). Anal. calcd %: C, 45.42; H, 3.81. Found: C, 45.52; H, 3.84. IR (CsI plate): 1677, 1655, 1603, 1570, 1572, 1376, 1252, 1109, 1010, 818 cm^{-1}.

Synthesis of $MeSi(p\text{-}C_6H_4CO_2H)_3$ (L2). A solution of $MeSi(p\text{-}C_6H_4Br)_3$ (1.0 g, 2.0 mmol) in 20 mL of THF was added dropwise to a solution of *n*-BuLi (2.5 M, 3.2 mL, 7.8 mmol) in 20 mL of THF at −78 °C and stirred at this temperature for a further 30 min. CO_2 was then bubbled through the cooled solution for 2 h, before warming to room temperature and stirring for an additional 18 h. The reaction was quenched by the addition of 50 mL of 1 M HCl. The organic layer was separated and washed with brine and dried over anhydrous $MgSO_4$. Removal of the solvents under a vacuum gave the crude product, which was recrystallized from hot EtOAc (approx 50 mL) to obtain pure $MeSi(p\text{-}C_6H_4CO_2H)_3$ (350 mg, 44%). Mp: >280 °C. ^{1}H NMR (d_6-DMSO) δ/ppm: 7.97 (d, J = 7.8 Hz, 6H, ArH), 7.62 (d, J = 7.8 Hz, 6H, ArH), 0.94 (s, 3H, CH_3).^{13}C NMR (d_6-DMSO) δ/ppm: 167.2 (CO_2H), 140.3 (Ar), 135.1 (ArH), 132.0 (Ar), 128.7 (ArH), −4.3 (CH_3). *m/e* (FAB): 405 $(M - H)^-$, 223, 153. Anal. calcd %: C, 65.01; H, 4.46. Found: C, 64.90; H, 4.42. IR (nujol mull): 2665, 2540, 1943, 1826, 1694, 1682, 1599, 1554, 1499, 1420, 1320, 1292, 1255, 1187, 1134, 1098, 1019, 934, 851, 784, 756, 731, 705 cm^{-1}.

Synthesis of $Me_2Si(p\text{-}C_6H_4CO_2H)_2$ (L3). A solution of $Me_2Si(p\text{-}C_6H_4Br)_2$ (10.0 g, 27 mmol) in 100 mL THF was added dropwise to a solution of *n*-BuLi (2.5 M in hexanes, 21.6 mL, 54 mmol) in 100 mL THF at −78 °C and stirred for 1 h. CO_2 was then bubbled through the stirred solution for a period of 2 h, before warming to room temperature and stirring for an additional 18 h. The reaction was quenched by addition of 50 mL 1 M HCl. The organic layer was separated, washed with brine and dried over anhydrous $MgSO_4$. The solvent was then removed by rotary evaporation to give the crude product, which was recrystallized from warm EtOAc to give $Me_2Si(p\text{-}C_6H_4CO_2H)_2$ (2.54 g, 31.3%). Mp: 285−288 °C. ^{1}H NMR (d_6-Acetone) δ/ppm: 8.05 (d, J = 8.0 Hz, 4H, ArH), 7.73 (d, J = 8.15 Hz, 4H, ArH), 0.67 (s, 6H, CH_3). ^{13}C NMR (d_6-Acetone) δ/ppm: 205.35 (CO_2H), 143.6 (Ar), 134.2 (ArH), 128.68 (ArH), −3.7 (CH_3). *m/e* (ES-): 300 $(M\text{-}H)^-$. Anal. Calcd. %: C 63.98, H 5.37; found C 63.90, H 5.43. IR (CsI plate): 3448, 2962, 2663, 2544, 1692, 1654, 1605, 1500, 1417, 1390, 1315, 1291, 1255, 1189, 1135, 1095, 1018, 941, 831, 803, 754, 709, 546, 506, 487, 342, 294 cm^{-1}.

Synthesis of $[Zn_4\{Si(C_6H_4CO_2)_4\}_2(H_2O)_5]\cdot(DMA)_{5.5}\cdot(H_2O)_{0.5}$ (1). A mixture of **L1** (20 mg, 0.04 mmol) and zinc(II) nitrate hexahydrate (50 mg, 0.08 mmol) in 10 mL of dimethylacetamide

(16) Liu, F. Q.; Tilley, T. D. *Inorg. Chem.* **1997**, *36*, 5090–5096.
(17) Liu, F. Q.; Tilley, T. D. *Chem. Commun.* **1998**, 103–104.
(18) Jung, O. S.; Kim, Y. J.; Kim, K. M.; Lee, Y. A. *J. Am. Chem. Soc.* **2002**, *124*, 7906–7907.
(19) Lee, J. W.; Kim, E. A.; Kim, Y. J.; Lee, Y. A.; Pak, Y.; Jung, O. S. *Inorg. Chem.* **2005**, *44*, 3151–3155.
(20) Lambert, J. B.; Liu, Z. Q.; Liu, C. Q. *Organometallics* **2008**, *27*, 1464–1469.
(21) Lambert, J. B.; Zhao, Y.; Stern, C. L. *J. Phys. Org. Chem.* **1997**, *10*, 229–232.
(22) Malek, N.; Maris, T.; Simard, M.; Wuest, J. D. *Acta Crystallogr., Sect. E* **2005**, *61*, O518−O520.
(23) Fournier, J. H.; Maris, T.; Wuest, J. D.; Guo, W. Z.; Galoppini, E. *J. Am. Chem. Soc.* **2003**, *125*, 1002–1006.
(24) El-Kaderi, H. M.; Hunt, J. R.; Mendoza-Cortes, J. L.; Cote, A. P.; Taylor, R. E.; O'Keeffe, M.; Yaghi, O. M. *Science* **2007**, *316*, 268–272.
(25) Rose, M.; Bohlmann, W.; Sabo, M.; Kaskel, S. *Chem. Commun.* **2008**, 2462–2464.
(26) Fournier, J. H.; Wang, X.; Wuest, J. D. *Can. J. Chem., Rev. Can. Chim.* **2003**, *81*, 376–380.

Table 1. Crystallographic Data for Compounds **1**, **2**, and **3**[a]

data	**1**	**2**	**3**
chemical formula	$C_{56}H_{42}O_{21}Si_2Zn_4$	$C_{32}H_{38}N_2O_9SiZn_2$	$C_{16}H_{15}O_5SiZn_{1.5}$
solvent	$5.5(C_4H_9NO)\cdot 0.5H_2O$	$0.5(C_5H_{11}NO)\cdot 0.5H_2O$	C_3H_7NO
fw	1856.74	813.06	486.52
T (°C)	−100	−100	−100
space group	*Pccn* (no. 56)	*I*2/*a* (no. 15)	$P\bar{1}$ (no. 2)
a (Å)	29.6302(2)	22.427(2)	6.3281(19)
b (Å)	22.57558(13)	14.597(3)	12.218(2)
c (Å)	28.20796(12)	25.232(3)	14.468(2)
α (deg)			112.071(4)
β (deg)		95.269(9)	99.440(5)
γ (deg)			97.528(19)
V (Å^3)	18868.84(19)	8225(2)	999.6(4)
Z	8[b]	8[b]	2[b]
ρ_{calcd} (g cm^{-3})	1.307	1.313	1.616
λ (Å)	1.54184[c]	1.54248[c]	0.71073[d]
μ (mm^{-1})	2.007	2.155	1.910
R_1[e]	0.074	0.069	0.030
wR_2[f]	0.227	0.200	0.073

[a] Refinements based on F^2. [b] All of the structures are polymeric, so the choice of formula (including solvent) and Z can be somewhat arbitrary, provided that the total contents of the unit cell equals the formula multiplied by Z. In each case here, the contents of the asymmetric unit were used as the formula. [c] Oxford Diffraction Xcalibur PX Ultra diffractometer. The different wavelengths reflect a realignment of the instrument. [d] Oxford Diffraction Xcalibur 3 diffractometer. [e] $R_1 = \sum||F_o| - |F_c||/\sum|F_o|$. [f] $wR_2 = \{\sum[w(F_o^2 - F_c^2)^2]/\sum[w(F_o^2)^2]\}^{1/2}$; $w^{-1} = \sigma^2(F_o^2) + (aP)^2 + bP$.

(DMA) and 10 mL of H_2O was heated to 100 °C in a sealed screw-top vial for 18 h. The mixture was allowed to cool to room temperature, and the resulting colorless crystals were removed from the reaction mixture by filtration. Yield = 21 mg (58%). Anal. calcd for $C_{56}H_{42}O_{21}Si_2Zn_4\cdot(H_2O)\cdot(C_4H_9NO)_5$ %: C, 50.31; H, 4.94; N, 3.86. Found: C, 50.36; H, 4.91; N, 3.91. Drying procedures for elemental analysis and X-ray crystallography differed so that there are minor differences in solvation. IR (ATR): 1598, 1541, 1498, 1395, 1203, 1188, 1098, 1018, 851, 773, 722, 704, 636, 591 cm^{-1}

Synthesis of $[Zn_2\{MeSi(C_6H_4CO_2)_3\}(OH)(DEF)_2]\cdot(DEF)_{0.5}\cdot(H_2O)_{0.5}$ (2). A mixture of **L2** (5 mg, 0.012 mmol) and zinc(II) nitrate hexahydrate (6 mg, 0.025 mmol) in 1 mL of diethylformamide (DEF) and 1 mL of H_2O was heated to 80 °C in a sealed screw-top vial for 24 h. The mixture was allowed to cool to room temperature to yield a small quantity (approximately 1 mg, 10%) of needlelike crystals which were removed from the reaction mixture by filtration. Anal. calcd for $C_{32}H_{38}N_2O_9SiZn_2\cdot(H_2O)_{0.5}(C_5H_{11}NO)_{0.5}$ %: C, 51.22; H, 5.54; N, 4.33. Found: C, 51.95; H, 5.60; N, 4.23. IR (ATR): 2978, 1611, 1640, 1544, 1498, 1395, 1309, 1263, 1214, 1102, 1021, 824, 794, 764, 741, 720, 704, 657 cm^{-1}.

Synthesis of $[Zn_{1.5}\{Me_2Si(C_6H_4CO_2)_2\}(OH)]\cdot DMF$ (3). A mixture of **L3** (60 mg, 0.2 mmol) and zinc(II) nitrate hexahydrate (70 mg, 0.30 mmol) in 7 mL of DMF and 1 mL of H_2O was heated to 100 °C in a sealed screw-top vial for 18 h. The mixture was allowed to cool to room temperature, and the resulting colorless crystals were removed from the reaction mixture by filtration. Yield = 83 mg (85%). Anal. calcd for $C_{32}H_{30}O_{10}Si_2Zn_3\cdot(C_3H_7NO)_2$ %: C, 47.20; H, 4.59; N, 2.90. Found: C, 47.16; H, 4.54; N, 2.92. IR (ATR): 1651, 1587, 1497, 1393, 1248, 1187, 1100, 1019, 911, 829, 806, 757, 721, 658, 597 cm^{-1}.

Physical Measurements. Thermal gravimetric analyses (TGA) were carried out using a Perkin-Elmer Pyris 1 machine, under a constant stream of dry nitrogen gas (flow rate, 20 mL min^{-1}) over a temperature range of 30−600 °C and at a heating rate of 5 °C min^{-1}.

Phase purity was confirmed using a Philips PW1700 series automated powder X-ray diffractometer with Cu Kα radiation and a graphite secondary crystal monochromator.

Single-Crystal X-Ray Crystallography. Table 1 provides a summary of the crystallographic data for compounds **1**, **2**, and **3**. Data were collected using Oxford Diffraction PX Ultra (**1** and **2**) and Xcalibur 3 (**3**) diffractometers, and the structures were refined based on F^2 using the SHELXTL and SHELX-97 program systems.[27] Full details of the X-ray structure solutions, including the handling of disorder present in the structures, are given in the Supporting Information. The CCDC numbers are 690295 to 690297, respectively.

Scheme 1. Synthesis of L1−L3

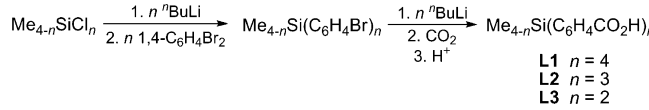

Results and Discussion

Synthesis of the Silicon-Based Connectors L1−L3. The tetra-acid connector Si(p-$C_6H_4CO_2H)_4$ (**L1**) was prepared from its tetra-bromo derivative according to literature procedures (Scheme 1).[26] The tri- and di-acid connectors MeSi(p-$C_6H_4CO_2H)_3$ (**L2**) and $Me_2Si(p$-$C_6H_4CO_2H)_2$ (**L3**) were also prepared using a similar synthetic protocol (Scheme 1). Although this is a new synthetic route to **L2** and **L3**, both have been previously prepared from the oxidation of their tolyl derivatives, MeSi(p-$C_6H_4Me)_3$[28] and $Me_2Si(p$-$C_6H_4Me)_2$,[29] respectively, and in addition in the case of **L3** from the hydrolysis of $Me_2Si(p$-$C_6H_4CN)_2$.[29]

Characterization of $[Zn_4\{Si(C_6H_4CO_2)_4\}_2(H_2O)_5]\cdot(DMA)_{5.5}\cdot(H_2O)_{0.5}$ (1). The reaction of tetra-acid **L1** with $Zn(NO_3)_2$ in DMA/H_2O (1:1) in a sealed vial at 100 °C for 18 h gave colorless needlelike crystals of $[Zn_4\{Si(C_6H_4CO_2)_4\}_2(H_2O)_5]\cdot(DMA)_{5.5}\cdot(H_2O)_{0.5}$ (**1**). Single-crystal diffraction studies on **1** reveal a 3D MOF material consisting of tetrahedral silicon-based connectors bridging distorted tetrahedral bimetallic SBUs (Figures 1 and 2).

It can therefore be seen that, during the MOF formation reaction, the **L1** connector undergoes deprotonation at each

(27) *SHELXTL PC*, version 5.1; Bruker ACS: Madison, WI, 1997. Sheldrick, G. *SHELX-97*; Institut Anorg. Chemie: Gottingen, Germany, 1998.
(28) Hopff, H.; Deuber, J. M.; Gallegra, P.; Said, A. *Helv. Chim. Acta* **1971**, *54*, 117–135.
(29) Speck, S. B. *J. Org. Chem.* **1953**, *18*, 1689.

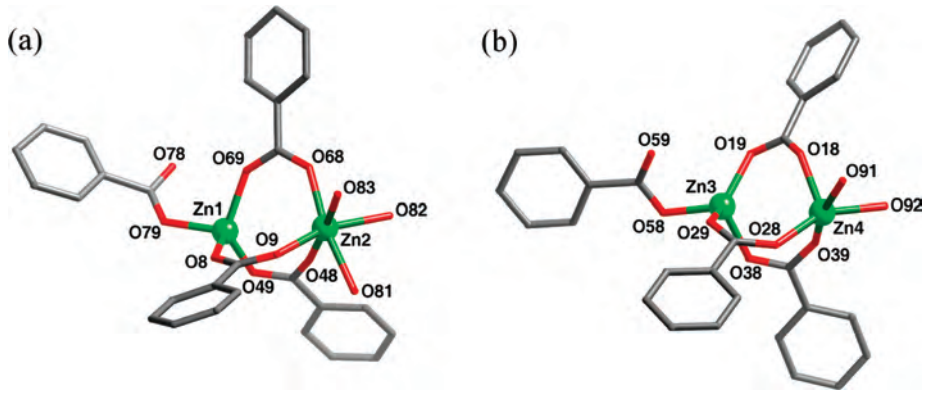

Figure 1. Ball-and-stick representation of the coordination environment about the two binuclear SBUs in **1**: (a) Zn1/Zn2 and (b) Zn3/Zn4. Crystallographic disorder is not shown, and hydrogen atoms have been omitted for clarity. Green = Zn, red = O, gray = C.

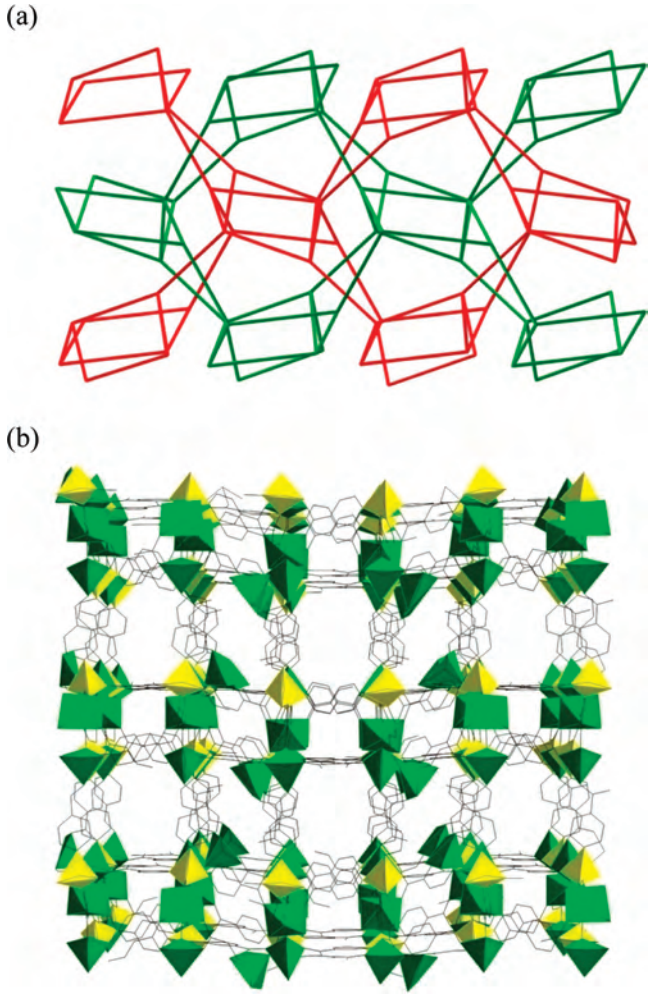

Figure 2. (a) Schematic representation of the 2-fold interpenetrated nets in **1** viewed along 100. (b) View of a section of **1** along 010. Noncoordinated solvent molecules and hydrogen atoms have been omitted for clarity. Green and yellow polyhedra represent the bonding environments of Zn and Si, respectively.

of its four carboxylic acid functionalities to give a tetra-anionic ligand. The SBUs in **1** form distorted tetrahedrons comprising two Zn(II) centers and four carboxylate groups. Two crystallographically distinct SBUs are present in the asymmetric unit of **1**, both of which suffer from some disorder in the crystal lattice (see the Supporting Information for full details). The major orientations for both SBUs are shown in Figure 1. The structure of **1** differs considerably from the only other reported MOF prepared from the same **L1** connector, $[Zn_2\{Si(C_6H_4CO_2)_4\}(H_2O)]$, which contains zinc-oxo chains as opposed to discrete SBUs, thus resulting in a very different overall topology.[20] This observed structural variability when using the same metal center and connecting unit can be can be rationalized by the differing reaction conditions (ratio of metal salt to acid, reaction temperature, and solvent system).

Both the Zn1/Zn2 and Zn3/Zn4 SBUs contain two zinc(II) centers bridged by three η^2-μ^2 carboxylate groups. Zn1 and Zn3 possess a tetrahedral environment completed by coordination to the oxygen anion of a fourth carboxylate group, with the remaining acid oxygen atom (O78/O59) being distal to the zinc centers. Zn−O distances for these tetrahedral metal centers lie in the range 1.915(5)−1.989(7) Å (mean 1.957 Å). The other zinc center in the SBU is coordinated by either three (Zn2) or two (Zn4) water molecules to give an octahedral or square-based pyramid environment, respectively. Mean $Zn-OH_2$ distances are 2.167 Å at the six-coordinate zinc (Zn2) and 2.062 Å at the five-coordinate zinc (Zn4).

Although binuclear $Zn_2(O_2CR)_4$-based SBUs are a relatively common motif in MOF chemistry, they usually form a paddlewheel conformation in which all four carboxylate groups symmetrically bridge the two metal centers to give a square nodal unit.[30,31] Nevertheless, tetrahedral SBUs similar to those in **1** have previously been reported in MOF-35[31] and MOF-47[30] as well as in several discrete cluster complexes.[32−34]

The overall structure of **1** is a distorted interpenetrating $SrAl_2$net of Schläfli notation $4^2.6^3.8$ (denoted: sra-c[35]) with both the silicon centers and bimetallic SBUs acting as nodal

(30) Braun, M. E.; Steffek, C. D.; Kim, J.; Rasmussen, P. G.; Yaghi, O. M. *Chem. Commun.* **2001**, 2532–2533.
(31) Kim, J.; Chen, B. L.; Reineke, T. M.; Li, H. L.; Eddaoudi, M.; Moler, D. B.; O'Keeffe, M.; Yaghi, O. M. *J. Am. Chem. Soc.* **2001**, *123*, 8239–8247.
(32) Klunker, J.; Biedermann, M.; Schafer, W.; Hartung, H. *Z. Anorg. Allg. Chem.* **1998**, *624*, 1503–1508.
(33) Darensbourg, D. J.; Wildeson, J. R.; Yarbrough, J. C. *Inorg. Chem.* **2002**, *41*, 973–980.
(34) Demirhan, F.; Gun, J.; Lev, O.; Modestov, A.; Poli, R.; Richard, P. *J. Chem. Soc., Dalton Trans.* **2002**, 2109–2111.
(35) Reticular Chemistry Structure Resource (RCSR) Web site of M. O'Keeffe. http://rcsr.anu.edu.au/ (accessed Sept. 2008).

points (Figure 2a). Although this topology is rare in MOF chemistry, it is not unprecedented.[36−38] Despite its interpenetrating nature, the structure is porous in all three dimensions, with crystallographic studies suggesting 5.5 DMA and 0.5 H_2O noncoordinated solvent molecules per asymmetric unit. Theoretical removal of these noncoordinated molecules gives a PLATON[39] (probe radius 1.2 Å) calculated solvent accessible void volume of 8973.7 $Å^3$ per unit cell or 47.6%. All of the channels in **1** are relatively narrow, with the largest channels running along the crystallographic 010 direction (see Figure 2b) having a rectangular cross section of ca. 7.5 × 5.5 Å.

Powder diffraction measurements show signals which closely match those of a simulated diffractogram based on the single-crystal X-ray data (see Figure S14), thus confirming the bulk purity of the product. TGA measurements on **1** show a 25.6% weight loss occuring in the temperature range 100−200 °C (see Figure S16). This is close to a predicted value of 26.2% for the loss of all noncoordinated solvents from **1** based on the X-ray crystallographic data. A further 40.3% weight loss occurs from 400−480 °C and can be attributed to decomposition of the MOF.

It is salient to note that the topology of **1** differs from that of $[Zn_2\{C(C_6H_4CO_2)_4\}(H_2O)_2]$ containing the analogous carbon-centered connector, in which paddlewheel-shaped $Zn_2(O_2CR)_4$ nodes give rise to square SBUs.[31] The move away from an idealized square SBU to a distorted tetrahedral SBU (as in **1**) has previously been attributed to increased steric demands of bulky carboxylate ligands around the bimetallic zinc unit.[30] However, in this case, there is no significant difference in the steric requirement of the silicon- and carbon-centered connectors, and the different SBUs adopted are probably best explained by minor changes in the thermodynamic and kinetic stabilities of the two networks caused by a combination of the differing reaction conditions and the longer Si−C bonds in **L1**. Precedent for this lies in the studies of Lambert et al. on Zn(II) MOFs with $M(C_6H_4CO_2)_4$ (M = C, Si, Ge) connectors, wherein large morphological differences in the MOF structures were attributed primarily to small changes in the ligand M−C bond distance.[20]

Characterization of $[Zn_2\{MeSi(C_6H_4CO_2)_3\}(OH)(DEF)_2]\cdot(DEF)_{0.5}\cdot(H_2O)_{0.5}$ (2). The reaction of tricarboxylic acid **L2** with $Zn(NO_3)_2$ in DEF/H_2O (1:1) in a sealed vial at 80 °C for 24 h gave columnar needlelike crystals. Single-crystal diffraction studies revealed these to be the 2D layered structure $[Zn_2\{MeSi(C_6H_4CO_2)_3\}(OH)(DEF)_2](DEF)_{0.5}\cdot(H_2O)_{0.5}$(**2**), comprising trigonal-pyramidal silicon-centered nodes and distorted octahedral tetra-nuclear zinc SBUs.

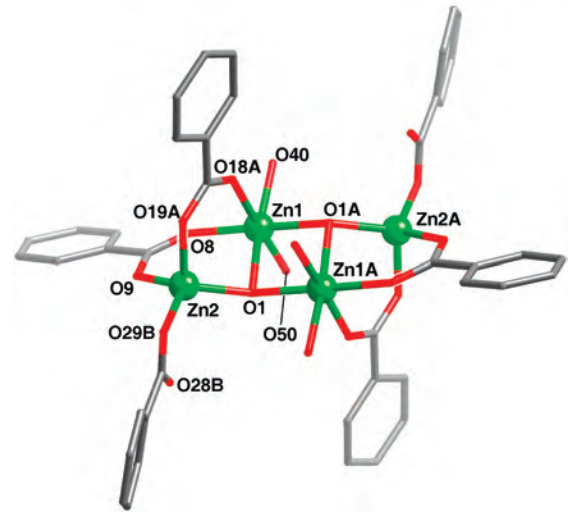

Figure 3. Ball-and-stick representation of the coordination environment about the tetranuclear SBU in **2**. Only the oxygen atoms of the DEF molecules are shown. Hydrogen atoms have been omitted for clarity. See Figure 1 caption for colors.

Each SBU in **2** sits on a crystallographic inversion center and comprises four Zn(II) cations, two hydroxyl groups, six carboxylate groups, and four coordinating DEF groups (Figure 3). Each O1 atom bridges three Zn centers with Zn−O1 distances of 2.093(3) (Zn1), 2.099(3) (Zn1A), and 1.953(3) Å (Zn2). The Zn−O−Zn angles around O1 (mean, 109.8°) are close to expected tetrahedral values, thus allowing the assignment of O1 as a μ^3-OH group,[40] as opposed to μ^3-oxo, which is known to exhibit a preference for the trigonal-planar conformation.[41] In addition, we were able to locate the hydroxo proton in the difference Fourier map. Of the six carboxylate groups, four are bidendate bridging and two are unidentate. Two crystallographically distinct Zn(II) atoms are present: Zn1, which is octahedral, with two hydroxyl groups, two bridging carboxylate groups, and two DEF molecules (Zn1−O in range 2.068(3)−2.110(5); mean 2.091 Å) and Zn2, which is tetrahedral, with one hydroxyl group, two bridging carboxylate groups, and one unidentate carboxylate group (Zn2−O in range 1.953(3)−1.964(4); mean 1.964 Å). The overall shape of the SBU is a distorted (compressed) octahedron. Similar $Zn_4(OH)_2L_6(solvent)_4$ motifs have been previously reported in both coordination polymers[42−45] and discrete complexes.[46]

These SBUs are joined together via the triply deprotonated **L2** ligands to give 2D layers with Schläfli notation $(4^6.6^6.8^3)(4^3)_2$ in which the topological term for the SBU is $4^6.6^6.8^3$ and that for the silicon center is 4^3 (Figure 4a). As

(36) Carlucci, L.; Ciani, G.; Macchi, P.; Proserpio, D. M.; Rizzato, S. *Chem.—Eur. J.* **1999**, *5*, 237–243.
(37) Wang, Q. M.; Guo, G. C.; Mak, T. C. W. *Chem. Commun.* **1999**, *1849*, 1850.
(38) Ferlay, S.; Koenig, S.; Hosseini, M. W.; Pansanel, J.; De Cian, A.; Kyritsakas, N. *Chem. Commun.* **2002**, 218–219.
(39) (a) Spek, A. L. *PLATON, A Multipurpose Crystallographic Tool*; Utrecht University: Utrecht, The Netherlands, 2008. (b) See also: Spek, A. L. *J. Appl. Crystallogr.* **2003**, *36*, 7–13.
(40) Vodak, D. T.; Braun, M. E.; Kim, J.; Eddaoudi, M.; Yaghi, O. M. *Chem. Commun.* **2001**, 2534–2535.
(41) Rosi, N. L.; Eddaoudi, M.; Kim, J.; O'Keeffe, M.; Yaghi, O. M. *Angew. Chem., Int. Ed.* **2002**, *41*, 284–287.
(42) Tao, J.; Tong, M. L.; Shi, J. X.; Chen, X. M.; Ng, S. W. *Chem. Commun.* **2000**, 2043–2044.
(43) Wang, R. H.; Hong, M. C.; Liang, Y. C.; Cao, R. *Acta Crystallogr., Sect. E* **2001**, *57*, m277–m279.
(44) Tao, J.; Yin, X.; Wei, Z. B.; Huang, R. B.; Zheng, L. S. *Eur. J. Inorg. Chem.* **2004**, *12*, 5–133.
(45) Gao, S.; Huo, L. H.; Gu, C. S.; Zhao, J. G.; Ng, S. W. *Acta Crystallogr., Sect. E* **2004**, *60*, m1331–m1333.
(46) Mukherjee, P. S.; Min, K. S.; Arif, A. M.; Stang, P. J. *Inorg. Chem.* **2004**, *43*, 6345–6350.

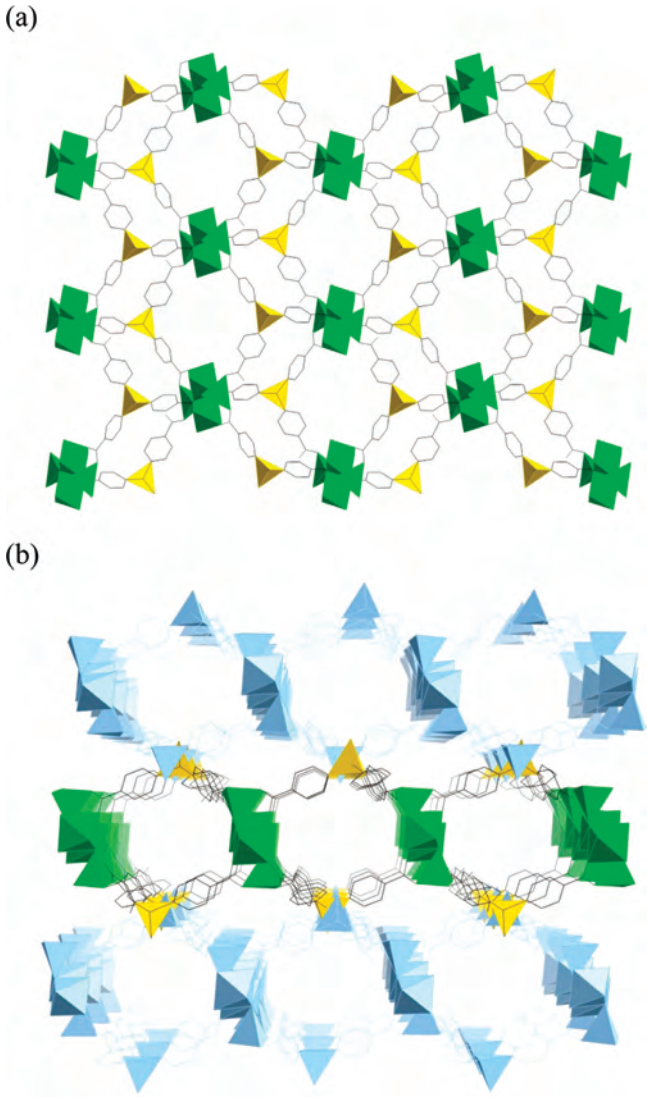

Figure 4. (a) View of the 2D layers parallel to the 101 plane in **2**. (b) The layers in **2** viewed along the 010 direction, highlighting the intercalation of adjacent layers. Hydrogen atoms and DEF molecules have been omitted for clarity. See Figure 2 caption for colors.

far as we are aware, this is the first example of this topology in MOF chemistry, although hydrogen-bonding nets have been reported which exhibit similar connectivity.[47,48] In contrast with more commonly used trigonal-planar tricarboxylate connecting units (such as 1,3,5-benzenetricarboxylate) which show a tendency to form 2D-planar layered materials, the incorporation of tripodal connectors in **2** leads to the formation of ridged 2D layers (Figure 4b). These layers intercalate with one another, with the methyl group on each silicon center being sited within a vacant cavity in an adjacent layer (Figure 4b). Small channels are observable within the structure along the crystallographic 100 and 010 vectors (see Figure 4b and Figure S1), with minimum rectangular cross sections of ca. 7.5 × 7.5 Å and 7.0 × 8.5 Å, respectively. Although these channels are mainly filled with coordinated DEF molecules, X-ray crystallographic studies also indicate

(47) Cordes, D. B.; Hanton, L. R.; Spicer, M. D. *J. Mol. Struct.* **2006**, *796*, 146–159.
(48) Cordes, D. B.; Hanton, L. R.; Spicer, M. D. *Cryst. Growth Des.* **2007**, *7*, 328–336.

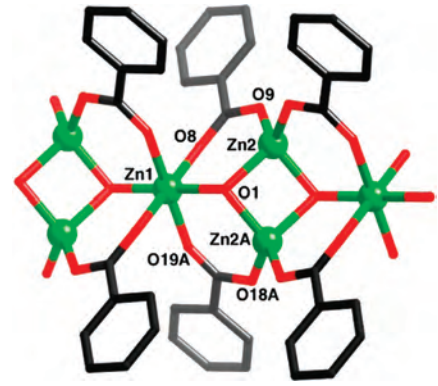

Figure 5. Ball-and-stick representation of the coordination environment about the zinc centers in **3**. Hydrogen atoms have been omitted for clarity. See Figure 1 caption for colors.

the presence of two included solvent molecules per SBU: one H_2O molecule sited within the intralayer channels and weakly hydrogen-bonded to the SBU hydroxo group ($O1\cdots OH_2$, 2.978(16) Å; $H\cdots O$, 2.13 Å; $O-H\cdots O$, 156°) and one DEF molecule sited between the layers. PLATON[39] calculations reveal a solvent-accessible void space of 2109.0 $Å^3$ per unit cell (25.6%) upon theoretical removal of the noncoordinated solvents. Due to its low yield, we have been unable to verify the bulk purity of **2** using powder diffraction experiments; however, unit cell determinations on several single crystals in the product were all consistent with **2**.

Characterization of $[Zn_{1.5}\{Me_2Si(C_6H_4CO_2)_2\}(OH)]\cdot$ DMF (3). Needlelike crystals of $[Zn_{1.5}\{Me_2Si(C_6H_4CO_2)_2\}$-$(OH)]\cdot$DMF (**3**) were obtained from the reaction of **L3** with $Zn(NO_3)_2$ in DMF/H_2O (7:1) in a sealed vial at 100 °C for 18 h. Single-crystal diffraction studies reveal the product (**3**) to adopt a 2D layered structure containing 1D zinc hydroxo chains within the layers.

In a manner similar to the synthesis of **2**, hydrothermal methods lead to the incorporation of hydroxo groups within the network structure of **3**. The O1 atom in **3** exhibits a trigonal-pyramidal coordination environment to three zinc centers (mean Zn−O−Zn bond angle of 107.5°), hence allowing its assignment as OH. In addition, we were able to locate the OH proton in the difference Fourier map. There are two crystallographically distinct zinc atoms within **3**: Zn1 is tetrahedral, with two hydroxo groups and two bridging carboxylate groups, and Zn2 is octahedral, with two hydroxo groups and four bridging carboxylate groups. Zn(1)−O distances about the octahedral center (range, 2.0705(13)−2.1124(13); mean, 2.097 Å) are, as expected, longer than those about the tetrahedral Zn(2) center (range, 1.9191(12)−1.9992(13); mean, 1.957 Å). All carboxylate groups adopt an η^2-μ^2 bidentate bridging coordination mode, resulting in the formation of a 1D Zn(OH) polymeric chain, a subsection of which is shown in Figure 5.

The zinc-hydroxo chains in **3** are interconnected through the dicarboxylate ligands to give 2D corrugated layers in which the $SiMe_2$ groups protrude both above and below the plane of the zinc atoms (Figure 6a). This gives rise to the formation of intralayer channels in the crystallographic 100 direction (Figure 6b) of approximate rectangular cross section 8.5 × 7.0 Å. DMF molecules are sited within these channels

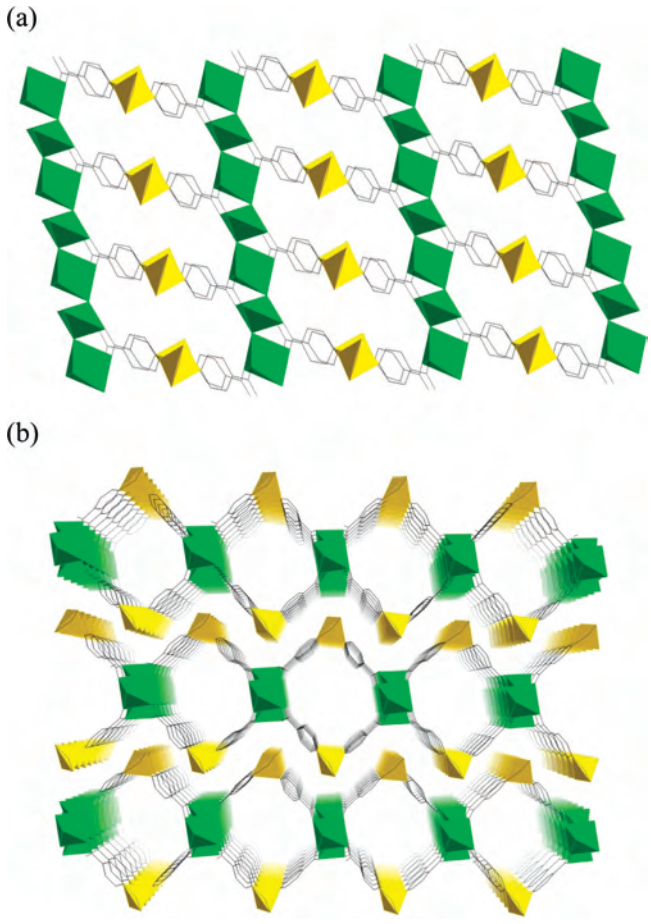

Figure 6. (a) View of the 2D layers parallel to the 001 plane in **3**. (b) The layers in **3** viewed along the 100 direction. Hydrogen atoms have been omitted for clarity. See Figure 2 caption for colors.

(one per lattice point) and form weak hydrogen bonds to the zinc hydroxyl group (O1···O, 2.8137(18) Å; H···O, 1.92 Å; O−H···O, 170°). The PLATON[39] (probe radius 1.2 Å) calculated solvent-accessible void volume for **3** after theoretical removal of these DMF molecules is 999.7 Å^3 per unit cell (23.9%). In contrast to the layers in **2**, the corrugated layers in **3** stack with alternate layers directly above one another, and no overlapping or intercalation of the layers is present.

The bulk purity of **3** was confirmed using powder diffraction measurements (Figure S15). TGA measurements show a 15.3% weight loss in the range 120−280 °C, which occurs in two distinct steps (Figure S17). This is consistent with the loss of the noncoordinated DMF from **3** (calcd, 15.0%). Further weight loss due to decomposition occurs above 420 °C.

Conclusion

In summary, we have been able to prepare and characterize three new Zn(II)-containing MOF materials based on a series of silicon-centered connecting units. These connecting units contain tetravalent silicon centers which have been functionalized to give either a tetra-, tri- or dicarboxylic acid—**L1**, **L2**, and **L3**, respectively. Although **L1**−**L3** are previously known compounds, a new route to **L2** and **L3** has been presented.

Reaction of the tetra-acid **L1** with Zn(II) centers gives MOF **1**—a 3D network material consisting of tetrahedral silicon-based connectors bridging distorted tetrahedral bimetallic SBUs. It can best be described as an interpenetrating $SrAl_2$ or sra-c net. Reaction of the tri- (**L2**) or dicarboxylic acids (**L3**) with Zn(II) metal centers give 2D layered materials, **2** and **3**, respectively. Compound **2** contains trigonal-pyramidal silicon-centered nodes connected to distorted octahedral tetranuclear SBUs, resulting in 2D layers of an unusual $(4^6.6^6.8^3).(4^3)_2$ topology which intercalate with one another. The 2D layers in **3** are built from bent silicon-based nodes and 1D zinc hydroxo chains to yield corrugated layers which stack with alternate layers directly above one another.

Together, these three new coordination polymers **1**−**3** demonstrate the potential versatility of tetrahedral-silicon-based connecting ligands for MOF construction. The synthetic accessibility of these connecting units, especially when compared to their carbon analogs, make them attractive targets for further investigation. Current research is focused upon variation of the aryl and methyl groups in **L1**−**L3** in order to confer different steric properties on these connecting units and to introduce new functional groups for designer-MOF construction.

Acknowledgment. This work was supported by the EPSRC (Grant EP/C528816/1) and has been conducted in association with the UK Energy Research Centre's programme of activity on "Materials for Advanced Energy Systems".

Supporting Information Available: View of the channels in **2** along the 100 direction (Figure S1), full details on the single-crystal structure determinations of **1**−**3** (Tables S1−S3 and Figures S2−S13), X-ray powder diffraction profiles for **1** and **3** (Figures S14 and S15), TGA traces for **1** and **3** (Figures S16 and S17), and X-ray crystallographic files (CIF). This material is available free of charge via the Internet at http://pubs.acs.org.

IC801174D